PROCEEDINGS OF THE ROYAL SOCIETY B

BIOLOGICAL SCIENCES

Out from under the wing: reconceptualizing the insect wing gene regulatory network as a versatile, general module for body-wall lobes in arthropods.

Journal:	Proceedings B			
Manuscript ID	RSPB-2021-1808.R2			
Article Type:	Research			
Date Submitted by the Author:	1 28-NOV-2021			
Complete List of Authors:	Fisher, Cera; University of Connecticut, Ecology and Evolutionary Biology Kratovil, Justin; University of Connecticut, Department of Ecology and Evolutionary Biology Angelini, David; Colby College, Biology Jockusch, Elizabeth; University of Connecticut, Ecology and Evolutionary Biology			
Subject:	Developmental biology < BIOLOGY, Evolution < BIOLOGY			
Keywords:	insect, gene, regulatory, networks, wing, homology			
Proceedings B category:	Evolution			

SCHOLARONE™ Manuscripts

Author-supplied statements

Relevant information will appear here if provided.

Ethics

Does your article include research that required ethical approval or permits?: This article does not present research with ethical considerations

Statement (if applicable):

CUST_IF_YES_ETHICS :No data available.

Data

It is a condition of publication that data, code and materials supporting your paper are made publicly available. Does your paper present new data?:

Yes

Statement (if applicable):

The raw scoring data used for this manuscript, along with the R code used to filter and collate the scoring data, are available on Data Dryad at https://doi.org/10.5061/dryad.wstqjq2n2 and are mirrored on GitHub at https://github.com/fishercera/oncopeltus_RNAI.

Conflict of interest

I/We declare we have no competing interests

Statement (if applicable):

CUST_STATE_CONFLICT : No data available.

- Out from under the wing: reconceptualizing the insect wing gene regulatory network as a versatile, general module for body-wall lobes in arthropods.
- 3 Cera R. Fisher¹, Justin D. Kratovil¹, David R. Angelini², and Elizabeth L.
- 4 Jockusch¹

6

7

8

9

10

11

12

13

14

15

16

17

18

19

20

21

22

23

24

- Department of Ecology and Evolutionary Biology, University of Connecticut, Storrs, CT, USA
- 2. Department of Biology, Colby College, Waterville, ME, USA

Abstract

Body plan evolution often occurs through the differentiation of serially homologous body parts, particularly in the evolution of arthropod body plans. Recently, homeotic transformations resulting from experimental manipulation of gene expression, along with comparative data on the expression and function of genes in the wing regulatory network, have provided a new perspective on an old question in insect evolution: how did the insect wing evolve? We investigated the metamorphic roles of a suite of ten wing- and body-wall-related genes in a hemimetabolous insect, Oncopeltus fasciatus. Our results indicate that genes involved in wing development in O. fasciatus play similar roles in the development of adult body-wall flattened cuticular evaginations. We found extensive functional similarity between the development of wings and other bilayered evaginations of the body wall. Overall, our results support the existence of a versatile development module for building bilayered cuticular epithelial structures that predates the evolutionary origin of wings. We explore the consequences of reconceptualizing the canonical wing-patterning network as a bilayered body-wall patterning network, including consequences for long-standing debates about wing homology, the origin of wings, and the origin of novel bilayered body-wall structures. We

conclude by presenting three testable predictions that result from this reconceptualization.

Introduction

One discovery of comparative developmental studies is that striking developmental similarity is frequently observed between morphologically divergent structures. Explanations for this observation fall into two classes of hypotheses: cooption and divergence of serial homologues. Co-option occurs when a gene is expressed in a new developmental context. Co-option resulting from the redeployment of an upstream regulatory gene may re-instantiate the expression of a suite of additional genes [1,2], resulting in the emergence of a new structure that does not have historical continuity with the structure from which the network was co-opted. There are now numerous examples of similar multi-component developmental networks that are deployed in non-homologous structures [3–7].

An alternative to co-option is the divergence of serial homologues. Serial homologues are body parts that are repeated across a developmental axis. Serial homology is thought to arise through repeated deployment of the same developmental network. These body parts often diverge during evolution but may retain similar developmental patterning networks because of their shared developmental history. In cases where new structures appear in the course of differentiation of serial homologues, the question naturally arises whether they are morphological manifestations of previously hidden variation, i.e., regions that were developmentally distinct but not morphologically distinct [8]. If so, the apparently new structures are expected to have serial homologues on other segments. Although these might be too divergent in

appearance to have been identified as homologous based on morphology alone, they would be expected to be identifiable via the other traditional homology criteria, such as similarity in development, position, and connectivity [9].

Recently, upstream regulators of the insect wing-patterning network have been found to be co-expressed in numerous additional (non-wing) structures across arthropods. These developmental similarities have revitalized long-standing debates about how wings originated [10,11] and about homology between wings and other arthropod structures [12,13]. Many of the apparently novel structures that express these genes share structural or architectural features with wings, in that they also comprise bilayered marginal outgrowths, including crustacean carapaces [14–16], mayfly [17] and crustacean gills [12,14], and treehopper helmets [18,19].

A wing-like gene regulatory network predates the origin of wings [12,14,16] and thus must have had an earlier function. An ancestral role in patterning body-wall margins was suggested by Shiga and colleagues based on gene expression in the *Daphnia* carapace [15]. The association of this gene regulatory network with margin outgrowths leads us to suggest that ancestrally, this gene regulatory network activated key architectural features of bilayered margins. Based on this, we hypothesize that deployment of this ancient gene regulatory network is more closely associated with an architectural feature of the body—bilayered cuticularized epithelium—regardless of where it occurs, than it is with a particular structure or position on the body. We tested this hypothesis using functional analyses of 10 "wing" and "body-wall" patterning genes in the large milkweed bug, *Oncopeltus fasciatus*, which possesses numerous bilayered epithelia, in both ancestrally conserved and novel positions (Fig 1A) [20–22]. Our results

suggest that developmental similarity between wings and body-wall outgrowths results from a versatile, re-deployable module that patterns bilayered epithelial outgrowths.

Methods

We chose a set of ten genes to investigate, based on the involvement of their orthologues in thoracic body-wall or wing development in the developmental genetic model organisms *Drosophila melanogaster* (Fig 1B) and *Tribolium castaneum*. We chose three of these genes—*apterous* (*ap*) [23], *vestigial* (*vg*) [24], and *nubbin* (*nub*) [25,26]—because they have been a focus of the wing serial homology debate [27–30]. Six additional genes were selected because of their interactions with these during body-wall or wing patterning: *homothorax* (*hth*) [31], *araucan/caupolican* (*ara/caup*) [32], *mirror* (*mirr*) [33], *tiptop/teashirt* (*tio*) [34], *tailup* (*tup*) [35], and *u-shaped* (*ush*) [36,37]. Finally, we included *serum response factor* (*srf*) (also known as *blistered*) because of its key function regulating apposition of basal membranes between bilayered epithelia in *Drosophila* [38,39]. Genes were identified in the *O. fasciatus* official gene set v1.2 [40] by reciprocal BLAST of *Drosophila* and *Tribolium* orthologues combined with tree-based methods using OrthoFinder (v2.3.1) [41].

After cloning and dsRNA synthesis, we followed established RNAi protocols for *O. fasciatus* [42], injecting 0.5-2 µg of dsRNA at both the 4th and 5th nymphal instars, with modifications in cases of high lethality. Specimens were preserved and scored for phenotypes across all thoracic body-wall and appendage regions. Representative specimens were photographed using a Canon EOS 6D DSLR camera attached to a Macropod Pro automated focus stacking apparatus (Macroscopic Solutions) with the right wing dissected off to show underlying meso- and metathoracic structures.

Composite (stacked) images were created from image batches using Zerene Stacker (v1.04). Additional details about cloning and RNAi protocols are provided in the supplemental methods and supplemental Tables 1-2.

Results

We scored phenotypes in 559 individuals (average 55.9 per gene, range of 37-86 total per gene, from two non-overlapping fragments) and 319 control specimens (Table 1). We present descriptive results for aberrant phenotypic traits in the thorax with a minimum penetrance of 15% among scorable adults. The supplemental materials contain descriptions of RNAi phenotypes in the head, genitalia, and wing bases. Penetrance for the thoracic regions focused on here is given in Table 1. The lethality of each gene target is in supplemental Table 3. In some cases, lower penetrance was accompanied by a higher death rate in experimental individuals than negative control individuals. This is particularly relevant for *ara/caup* RNAi, for which the second fragment resulted in 0% survival, suggesting that for this gene, the strongest phenotypes were lethal.

All thoracic bilayered layered epithelia in *Oncopeltus* require *srf*

RNAi targeting *srf* in *Oncopeltus* caused bilayered epithelia to fill with hemolymph and balloon out. This "blistering" phenotype occurred not only in the wings (Fig 2C,D), but also in bilayered body-wall regions: the posterior pleural margins of all three thoracic segments, the supracoxal lobes of the first and second thoracic segments, an anterior extension of the pronotum (first thoracic segment) called the collar, the posterior margin of the pronotum, and a large posterior extension of the second thoracic segment (the

mesoscutellum) (Fig 3C, 4C, S2). All genes that affect the same regions as *srf* are therefore associated with bilayered epithelial outgrowths.

"Wing" gene RNAi phenotypes reveal similarities in patterning of wings and bilayered body-wall epithelia.

We recovered wing phenotypes that closely resemble those previously described by Medved et al. [43] for three canonical wing-patterning genes, *ap*, *nub*, and *vg*. Phenotypes were milder than often observed in *Drosophila*, as expected for a hemimetabolous insect where wing primordia develop externally over multiple juvenile stages. In *nub* and *vg* RNAi specimens, the wings were severely reduced in size (Fig. 2E,F). In *nub* RNAi specimens, the proximal region was more severely affected than the distal region, while the size reduction was more even over the whole wing blade in *vg* RNAi specimens. *vg* RNAi specimens also had distally fused wing veins (Fig 2F). RNAi targeting *ap* did not result in size or shape changes. However, the corium of the forewing was desclerotized, becoming thin and membranous, and the wing veins in the membranous forewing were not stiffened or pigmented, leaving a cleared outline where there would be dark veins in the wild-type (Fig 2D), a phenotype reminiscent of *Tribolium ap* RNAi elytra phenotypes [44].

Two regions of thoracic bilayered body-wall, the posterior pronotal lobe (Fig. 3) and the posterior pleural margins (Fig. 4), required the key wing genes vg, ap, and nub for normal development in *Oncopeltus*. Furthermore, knockdown phenotypes suggested that their body-wall development roles resemble their wing development roles. Reductions of the posterior pleural margins of all three thoracic segments were most pronounced in response to nub RNAi (Fig 4E, supplemental Fig S3). In vg RNAi

specimens, a reduction in a small area comprising the junction between the pleural and tergal part of the prothorax resulted in a sinuous curvature of the propleural margin (Fig 4F, supplemental Fig S3). *nub* RNAi also caused the greatest reduction in the posterior pronotum (also described by ref. [43]), with *vg* and severely affected *ap* RNAi specimens showing similar effects to *nub*. This reduction exposes the wing hinge and portions of the mesonotum that are normally hidden by the pronotum (Fig 3E,F). Like the wings, the pleural lobes of *ap* RNAi specimens appeared to retain wild-type size and shape, but their texture was affected; they were thinner and more flexible, a characteristic usually accompanied by decreased melanization (Fig 4D).

Development of the scutellum was also altered in response to depletion of all three wing genes; however, the phenotypic effects differed substantially across genes and was qualitatively different from the effects in the wings, pleural margins, and posterior pronotal lobe. Knockdown of *vg* resulted in the scutellum of these specimens having a broadened posterior edge (Fig 3F). *ap* RNAi resulted in a dorsally upturned scutellum (Fig 4D; supplemental Fig S4). The scutellum in *nub* RNAi specimens appeared flatter than in wild-type specimens when viewed laterally (Fig 4E), although it retained a triangular shape dorsally (Fig 3E).

The other two bilayered epithelia each required a subset of the core wing genes for normal development. The collar was reduced in *nub* (11 of 51; 22% penetrance) and *ap* (20 of 86 specimens; 23% penetrance) RNAi specimens (Fig 3E,D), leaving a gap between the collar and eyes and exposing the posterior head. This phenotype was also observed at very low frequency (3 of 48; 6% penetrance) in *vg* RNAi specimens (Table 1). The supracoxal lobes of the prothorax and mesothorax were affected by knockdown

of *nub* (Fig 4E), but not *vg* or *ap*. The reduction in these lobes resulted in a more open coxal cleft (also described by ref. [43]).

Functional comparison of "body-wall" genes in bilayered epithelia reveals wing and nonwing roles

Several of the genes we selected because of their previously described roles in body-wall development were required for normal wing development in *Oncopeltus*. *Mirr* RNAi wings lacked the sharp separation between the clavus/anal lobe and the rest of the wing blade (Fig 2I). Depletion of *hth* resulted in a subtle change to the curvature of the anterior margin of both wings (Fig 2G). Mild depigmentation was observed in *tup* RNAi specimens, in which the normally black intervein regions of the distal forewing were lighter or clear (Fig 2J).

Normal development of the scutellum, collar, posterior pronotal lobe, and posterior pleural lobes required all of the "body-wall" genes we investigated (*ara/caup*, *hth*, *mirr*, *tio*, *tup*, *ush*; see supplemental Fig S6 for a larger sample of normal *GFP* RNAi phenotypes). The scutellum was mildly affected by RNAi targeting *ara/caup* and *hth* (Fig 3G-H), and severely affected by RNAi targeting *mirr*, *tup*, *tio*, and *ush*, losing the wild-type triangular shape (Fig 3I-L, Fig 4I-L). The collar was reduced in *ara/caup*, *hth*, *mirr*, *tio*, *tup*, and *ush* RNAi, resulting in a gap between the collar and the back of the eyes (Fig 3G-H,J-L). Knockdown of *ara/caup*, *hth*, *mirr*, *tio*, and *ush* produced smaller pronota, resulting from reduction or folding of the posterior pronotal lobe, revealing the wing base and characters of the mesonotum normally hidden by the pronotum (Fig 3G-I,K-L). *tup* RNAi specimens lacked lateral sculpting in the pronotum (Fig. 3H).

The most severe reduction of the pleural region was observed in response to *tio* knockdown; individuals that survived to adulthood lacked both the posterior pleural lobes and supracoxal lobes, retaining only the single-layered portion of the pleural plates (Fig 4K). The pleural margins of *hth*, *mirr*, and *tup* RNAi were reduced, with the most obvious reduction occurring along the anterior-posterior axis (Fig 4H-J). Additionally, the metapleuron (T3) was rounded in the dorsal posterior corner (Fig 4H-J), whereas in wild-type individuals, it is squared off (Fig 4B). In RNAi for *ush*, the metapleuron was shorter in the dorso-ventral axis than in the wild-type. RNAi targeting *ara/caup*, *hth*, and *tio* led to open supracoxal clefts (Fig 4G,H,K, supplemental Fig S5).

Discussion

A structural framework

Understanding of pathways involved in the developmental patterning of arthropods is historically contingent upon discoveries in the resource-abundant *Drosophila* system. *vestigial*, *apterous*, and *nubbin* were all named for their dramatic wing-mutant phenotypes in *Drosophila* [23–25,45,46] and are central to the conserved wing-patterning network [47]. In particular, *vg* became entrenched as a "wing gene" because of its ability to induce wing-like outgrowths in other parts of the fly when ectopically expressed [48], because phenotypes of regulatory mutants were confined to the wings [49], and because it activates expression of downstream genes in the wing-patterning network, including *nub* and *srf* [27].

Subsequently, when comparative data on expression and function of *vg* (and other components of the wing regulatory network) in other arthropods showed phenotypes in other, non-wing body parts [27–29], these parts were interpreted as wing

homologues or wing serial homologues, depending on where they occurred. For example, under knockdown of the HOX gene *Sex-combs reduced*, the prothoracic tissues that give rise to homeotic wings express and require components of the wing regulatory network, including vg, nub, and ap [28]. We note that Drosophila lacks extensive cuticularized bilayered epithelia outside the wings (Fig 1B); this is a derived phenotype within insects, which had multiple regions of bilayered body wall ancestrally. Consequently, any genes with general functions in bilayered epithelia would have been identified as wing-specific from genetic studies in Drosophila.

Sets of "wing" and "body-wall" genes produce similar phenotypes in bilayered structures

This study examined the effects of genes traditionally considered to be "wing" genes (*vg*, *ap*, *nub*), as well as genes more commonly thought of as body-wall patterning genes. Similar knockdown phenotypes across diverse structures for sets of "wing" and "body-wall" genes highlight their shared roles in patterning marginal outgrowths. For example, knockdown of *nub*, *hth*, and *mirr* produced similar reductions of the posterior pleural margins (Fig 4). The collar was reduced in *ara/caup*, *hth*, *tup*, *tio*, and *ush* knockdown, exposing the back of the head, resembling the *nub* and *ap* phenotypes (Fig 3). The reduction of the supracoxal lobes, resulting in a more open coxal cleft, was present in *ara/caup*, *hth*, and *tio* RNAi phenotypes and resembled the *nub* RNAi phenotypes (Fig 4).

Our results demonstrate that the bilayered margins of the thoracic body-wall are regulated by a shared set of genes, including the canonical wing genes, regardless of their anatomical position. This set of genes operates in the supracoxal lobes, the posterior pleural lobes, the posterior pronotal lobe, and the anterior collar, in addition to

the wings. In light of these results, we are motivated to reconceptualize the wingpatterning gene regulatory network. Rather than define the developmental function of
this genetic module as wing patterning, we conclude that it is more reflective of its
evolutionary history to describe the shared function of these genes based on the shared
structural similarity of these characters. We propose that these genes are part of a
developmental network that regulates the growth and three-dimensional patterning of
bilayered, cuticularized body-wall outgrowths—a character type that includes wings and
many other structures.

Ancestral function of the wing-patterning network in body-wall lobes and consequences for the debate about the origin of insect wings

Four observations motivated the hypothesis that the ancestral function of the wing-patterning network described from *Drosophila* is ancestrally responsible for the patterning of bilayered epithelial margins (this paper and refs. [14,16]). The first is that the network is evolutionarily older than wings, as shown by the spatial expression patterns of key components in a primitively wingless insect [50]. The second observation is that *vg*, *nub*, *ap*, and *wingless* (*wg*), or subsets thereof, are prominently expressed at the developing dorsal body wall margins of many insects and crustaceans [14,16]. Third, late Cambrian fossils show that bilayered margins arose early in arthropod evolution and were likely present posteriorly in body-wall segments and distally in limb segments [51]. Finally, this network has been found to be active in insect wings, in the gills of mayflies [52], crustaceans [14,16] and horseshoe crabs [53], in the *Daphnia* carapace [15,54], and in treehopper helmets [18,19]. All of these structures are bilayered epithelia.

Reconceptualizing the wing-patterning network as a bilayered margin patterning network provides a new framework that we believe helps resolve some debates about homology (both serial homology within a single organism and special homology between species). For example, shared expression or function of this gene regulatory network likely indicates that the structures share homology as bilayered epithelia (in the same way that bird wings and bat wings are homologous as tetrapod limbs), but is not sufficient to indicate a closer evolutionary connection as wings.

According to this view, diverse arthropod structures all share an identity as bilayered epithelia, including insect wings; the gills of crustaceans, chelicerates, and mayflies; treehopper helmets; abdominal gin traps in beetle pupae; and marginal outgrowths of body and limb segments. However, the widespread occurrence of bilayered epithelia means that developmental similarity resulting from the use of this gene-regulatory network does not provide direct evidence of either special homology or serial homology in the classic sense of being repeated structures at the same position along a body axis. Instead, bilayered margins may be serially homologous in the way that structures such as sensory bristles are, which can develop at a wide array of body locations [55].

This interpretation has consequences for the debate about the origin of insect wings. Central to this debate is the interpretation of structures on non-winged segments of insects as wing serial homologues [27–29,56], and of ancestral limb structures of non-winged arthropods as homologs of and precursors to wings [14,16]. Our interpretation predicts that bilayered body-wall evaginations throughout the body are likely to share developmental dynamics and thus gene expression. Under this

interpretation, additional evidence, such as conserved markers of distinct marginal identities that predate the origin of wings, would be needed to support these inferences about homology to wings.

Our view helps resolve a divide in the literature about how developmental similarities resulting from shared deployment of the bilayered epithelium regulatory network are interpreted [57]. Those who focus on the serial homology explanation are have generally studying structures that, like wings, emerge along a restricted region of the lateral tergal margins [14,29]. This similarity in position reflects one of the other traditional criteria for identifying homologues [9]. Those who favor the co-option explanation are focused on traits with an extensive margin, encompassing non-lateral regions. Because the wing-like developmental network is deployed in a different position along the body axis than it is in wings, they conclude that the structures lack serial homology at the anatomical level, and so attribute the developmental genetic similarity to co-option [15,18,58]. In our view, both interpretations are partially correct: shared similarity results from a shared ancestral function of the developmental network, but it does not indicate serial homology as anything more than bilayered epithelia. Our data from *Oncopeltus* show that this genetic module functions in anterior and posterior pleural margins that have never been suggested to be serially homologous to wings because of their segmental position (i.e., presence on wing-bearing segments). Thus, a clear division between wing and body-wall grounded in gene expression or function is elusive.

This change in framework also helps explain some details of developmental phenomena that are incongruent with the serial homology framework. For example,

276

277

278

279

280

281

282

283

284

285

286

287

288

289

290

291

292

293

294

295

296

297

300

301

302

303

304

305

306

307

308

309

310

311

312

313

314

315

316

317

318

319

320

321

during embryonic development, vg, wg, and ap are expressed not only along the lateral and posterior margins of the developing segments, but also across the anterior margin of the pronotum (but not more posterior segments). This pattern is present in *Tribolium* (beetle) [28,59], Gryllus (cricket) [60], and Parhyale (crustacean) [14,61]. Under the wing serial homologue framework, the posterolateral tergal margins could potentially be interpreted as cryptic wing serial homologues (i.e., tissues that could develop into wings but are repressed), but the anterior pronotal margin cannot. Under our proposed framework, the anterior pronotal margin is simply one more region of flattened marginal outgrowths, exemplified in this study by the milkweed bug collar. In the beetle Onthophagus, putative wing serial homologues—the dorsal support structures—have been characterized on parts of segments that already bear wings [56]. Under our proposed framework, rather than being serially homologous qua wings, these structures are serially homologous qua bilayered epithelial outgrowths. They share developmental similarity with wings because both use the ancestral regulatory network for the development of bilayered cuticularized outgrowths.

Predictions and hypothesis testing

Three testable predictions follow from our hypothesis that deployment of the network is closely linked to the bilayered architecture of these margins. First, the network is predicted to be highly conserved in bilayered margins that have been continuously present in arthropod history. This includes the bilayered margin that forms the insect wing. Second, where morphological evolution has resulted in replacement of bilayered margins by single-layered margins (e.g., as in the thoracic body-wall of *Drosophila*), we predict that expression of the ancestral wing patterning network has

been modified or that its function has been suppressed. Third, we predict that novel bilayered body-wall outgrowths are likely to be patterned by this developmental network. This prediction is directly supported by the results in this study: the evaginated mesoscutellar lobe is a synapomorphy of heteropterans [22], is bilayered, and requires core elements of this network, including *ap*, *nub*, and *vg*, for proper development. It is also supported by studies of the novel, bilayered prothoracic helmet of treehoppers [18,19]. Viewed through this framework, it is possible that many cases of novel bodywall outgrowths that have been characterized variously as wing serial homologues or as cases of co-option may be resolved as developmentally similar due to shared architectural features.

Data and Code Availability

The raw scoring data used for this manuscript, along with the R code used to filter and collate the scoring data, are available on Data Dryad at https://doi.org/10.5061/dryad.wstqjq2n2 and are mirrored on GitHub at https://github.com/fishercera/oncopeltus RNAI.

Acknowledgments

Funding for this project was provided by a grant from the National Science

Foundation to ELJ (NSF IOS 1656572), a grant from the University of Connecticut

Department of Ecology and Evolutionary Biology to CRF, and an award from the EvoDevo-Eco Network (EDEN RCN, NSF IOS 0955517) to CRF. CRF was supported by an

Outstanding Scholar Fellowship from the University of Connecticut during portions of
this work. We appreciate the assistance of Adam Chiu, Katherine Starr, and Ariana

Rojas in bug care and RNAi experiments. We appreciate very helpful feedback from

346

347

348

349

350

351

352

353

Ariel Chipman and an anonymous reviewer. An earlier version of this manuscript benefited from comments by David Wagner, Charles Henry, and Yaowu Yuan.

Author contributions

CRF and ELJ conceived the project, and JDK contributed to project design. CRF and DRA developed the RNAi protocol from DRA's current laboratory techniques, and DRA contributed several plasmids. CRF and JDK generated and scored the RNAi data; all authors contributed to data interpretation. CRF wrote the first draft of the manuscript. ELJ, JDK, DRA, and CRF revised the manuscript.

References

- Koshikawa S. 2015 Enhancer modularity and the evolution of new traits. *Fly (Austin)* 9, 155–159. (doi:10.1080/19336934.2016.1151129)
- 2. Monteiro A. 2012 Gene regulatory networks reused to build novel traits: Co-option of an eye-related gene regulatory network in eye-like organs and red wing patches on insect wings is suggested by *optix* expression. *BioEssays* **34**, 181–186. (doi:10.1002/bies.201100160)
- 36. Glassford WJ, Johnson WC, Dall NR, Smith SJ, Liu Y, Boll W, Noll M, Rebeiz M. 2015 Co-option of an ancestral Hox-regulated network underlies a recently evolved morphological novelty. *Dev. Cell* **34**, 520–531. (doi:10.1016/j.devcel.2015.08.005)
- 4. Lemons D, Fritzenwanker JH, Gerhart J, Lowe CJ, McGinnis W. 2010 Co-option of an anteroposterior head axis patterning system for proximodistal patterning of appendages in early bilaterian evolution. *Dev. Biol.* **344**, 358–362. (doi:10.1016/j.ydbio.2010.04.022)
- Linz DM, Hu Y, Moczek AP. 2019 The origins of novelty from within the confines of homology: the developmental evolution of the digging tibia of dung beetles. *Proc. R. Soc. B Biol. Sci.* 286, 20182427. (doi:10.1098/rspb.2018.2427)
- Martin A, McCulloch KJ, Patel NH, Briscoe AD, Gilbert LE, Reed RD. 2014 Multiple
 recent co-options of Optix associated with novel traits in adaptive butterfly wing
 radiations. *EvoDevo* 5, 7. (doi:10.1186/2041-9139-5-7)
- 7. Reed RD *et al.* 2011 *optix* drives the repeated convergent evolution of butterfly wing pattern mimicry. *Science* **333**, 1137–1141. (doi:10.1126/science.1208227)
- Wagner GP. 2014 Homology, Genes, and Evolutionary Innovation. Princeton, NJ:
 Princeton University Press.
- Owen R. 1848 On the Archetype and Homologies of the Vertebrate Skeleton.
 London: Richard and John E. Taylor.
- 10. Crampton G. 1916 The phylogenetic origin and the nature of the wings of insects according to the paranotal theory. *J. N. Y. Entomol. Soc.* **24**, 1–39.
- 11. Kukalová-Peck J. 1983 Origin of the insect wing and wing articulation from the arthropodan leg. *Can. J. Zool.* **61**, 1618–1669. (doi:10.1139/z83-217)
- 12. Averof M, Cohen SM. 1997 Evolutionary origin of insect wings from ancestral gills.

 Nature 385, 627–630. (doi:10.1038/385627a0)
- 386 13. Carroll SB, Weatherbee SD, Langeland JA. 1995 Homeotic genes and the 387 regulation and evolution of insect wing number. *Nature* **375**, 58–61. 388 (doi:10.1038/375058a0)

- 14. Clark-Hachtel CM, Tomoyasu Y. 2020 Two sets of candidate crustacean wing homologues and their implication for the origin of insect wings. *Nat. Ecol. Evol.* **4**, 1694–1702. (doi:10.1038/s41559-020-1257-8)
- 15. Shiga Y, Kato Y, Aragane-Nomura Y, Haraguchi T, Saridaki T, Watanabe H, Iguchi
 T, Yamagata H, Averof M. 2017 Repeated co-option of a conserved gene regulatory
 module underpins the evolution of the crustacean carapace, insect wings and other
 flat outgrowths. *Prepr. BioRxiv* (doi:10.1101/160010)
- 396 16. Bruce HS, Patel NH. 2020 Knockout of crustacean leg patterning genes suggests 397 that insect wings and body walls evolved from ancient leg segments. *Nat. Ecol.* 398 *Evol.* **4**, 1703–1712. (doi:10.1038/s41559-020-01349-0)
- 17. Almudi I, Martín-Blanco CA, García-Fernandez IM, López-Catalina A, Davie K, Aerts
 S, Casares F. 2019 Establishment of the mayfly *Cloeon dipterum* as a new model
 system to investigate insect evolution. *EvoDevo* 10, 6. (doi:10.1186/s13227-019-0120-y)
- 403 18. Fisher CR, Wegrzyn JL, Jockusch EL. 2020 Co-option of wing-patterning genes
 404 underlies the evolution of the treehopper helmet. *Nat. Ecol. Evol.* 4, 250–260.
 405 (doi:10.1038/s41559-019-1054-4)
- 406 19. Prud'homme B, Minervino C, Hocine M, Cande JD, Aouane A, Dufour HD, Kassner VA, Gompel N. 2011 Body plan innovation in treehoppers through the evolution of an extra wing-like appendage. *Nature* **473**, 83–86. (doi:10.1038/nature09977)
- 409 20. Bramer C, Friedrich F, Dobler S. 2017 Defence by plant toxins in milkweed bugs
 410 (Heteroptera: Lygaeinae) through the evolution of a sophisticated storage
 411 compartment. Syst. Entomol. 42, 15–30. (doi:10.1111/syen.12189)
- 412 21. Govind CK, Dandy JWT. 1970 The thoracic mechanism of the milkweed bug,
 413 Oncopeltus fasciatus (Heteroptera: Lygaeidae). Can. Entomol. 102, 1057–1074.
 414 (doi:10.4039/Ent1021057-9)
- 22. Matsuda R. 1970 Morphology and evolution of the insect thorax. *Mem. Entomol.*Soc. Can. 102, 5–431. (doi:10.4039/entm10276fv)
- 23. Cohen B, McGuffin ME, Pfeifle C, Segal D, Cohen SM. 1992 *apterous*, a gene required for imaginal disc development in *Drosophila* encodes a member of the LIM family of developmental regulatory proteins. *Genes Dev.* 6, 715–729.
 (doi:10.1101/gad.6.5.715)
- 421 24. Williams JA, Paddock SW, Vorwerk K, Carroll SB. 1994 Organization of wing
 422 formation and induction of a wing-patterning gene at the dorsal/ventral compartment
 423 boundary. *Nature* 368, 299–305. (doi:10.1038/368299a0)

- 424 25. Cifuentes FJ, Garcia-Bellido A. 1997 Proximo-distal specification in the wing disc of
- 425 Drosophila by the nubbin gene. Proc. Natl. Acad. Sci. 94, 11405–11410.
- 426 (doi:10.1073/pnas.94.21.11405)
- 427 26. Ng M, Diaz-Benjumea FJ, Cohen SM. 1995 *nubbin* encodes a POU-domain protein
- required for proximal-distal patterning in the *Drosophila* wing. *Development* **121**,
- 429 589–599. (doi:10.1242/dev.121.2.589)
- 430 27. Hu Y, Linz DM, Moczek AP. 2019 Beetle horns evolved from wing serial homologs.
- 431 *Science* **366**, 1004–1007. (doi:10.1126/science.aaw2980)
- 432 28. Clark-Hachtel CM, Linz DM, Tomoyasu Y. 2013 Insights into insect wing origin
- provided by functional analysis of *vestigial* in the red flour beetle, *Tribolium*
- 434 castaneum. Proc. Natl. Acad. Sci. **110**, 16951–16956.
- 435 (doi:10.1073/pnas.1304332110)
- 436 29. Ohde T, Yaginuma T, Niimi T. 2013 Insect morphological diversification through the
- modification of wing serial homologs. *Science* **340**, 495–498.
- 438 (doi:10.1126/science.1234219)
- 439 30. Tomoyasu Y, Ohde T, Clark-Hachtel C. 2017 What serial homologs can tell us about
- the origin of insect wings. *F1000Research* **6**, 268.
- 441 (doi:10.12688/f1000research.10285.1)
- 31. Smith FW, Jockusch EL. 2014 Hox genes require *homothorax* and *extradenticle* for
- body wall identity specification but not for appendage identity specification during
- metamorphosis of *Tribolium castaneum*. Dev. Biol. **395**, 182–197.
- 445 (doi:10.1016/j.ydbio.2014.08.017)
- 446 32. del Corral RD, Aroca P, Gomez-Skarmeta JL, Cavodeassi F, Modolell J. 1999 The
- 447 Iroquois homeodomain proteins are required to specify body wall identity in
- 448 *Drosophila. Genes Dev.* **13**, 1754–1761. (doi:10.1101/gad.13.13.1754)
- 33. Ikmi A, Netter S, Coen D. 2008 Prepatterning the *Drosophila* notum: The three
- 450 genes of the *iroquois* complex play intrinsically distinct roles. *Dev. Biol.* **317**, 634–
- 451 648. (doi:10.1016/j.ydbio.2007.12.034)
- 452 34. Shippy TD, Tomoyasu Y, Nie W, Brown SJ, Denell RE. 2008 Do *teashirt* family
- 453 genes specify trunk identity? Insights from the single tiptop/teashirt homolog of
- 454 Tribolium castaneum. Dev. Genes Evol. **218**, 141–152. (doi:10.1007/s00427-008-
- 455 0212-5)
- 456 35. de Navascues J, Modolell J. 2007 *tailup*, a LIM-HD gene, and Iro-C cooperate in
- 457 Drosophila dorsal mesothorax specification. Development **134**, 1779–1788.
- 458 (doi:10.1242/dev.02844)



- 36. Sato M, Saigo K. 2000 Involvement of *pannier* and *u-shaped* in regulation of Decapentaplegic-dependent *wingless* expression in developing *Drosophila* notum. *Mech. Dev.* **93**, 127–138. (doi:10.1016/S0925-4773(00)00282-3)
- 37. Tomoyasu Y, Ueno N, Nakamura M. 2000 The Decapentaplegic morphogen gradient regulates the notal *wingless* expression through induction of *pannier* and *u-shaped* in Drosophila. *Mech. Dev.* **96**, 37–49. (doi:10.1016/S0925-4773(00)00374-9)
- 38. Fristrom D, Gotwals P, Eaton S, Kornberg TB, Sturtevant M, Bier E, Fristrom JW.
 1994 *blistered*: a gene required for vein/intervein formation in wings of *Drosophila*.
 Dev. Camb. Engl. 120, 2661–2671.
- 468 39. Montagne J, Groppe J, Guillemin K, Krasnow MA, Gehring WJ, Affolter M. 1996 The
 469 *Drosophila* Serum Response Factor gene is required for the formation of intervein
 470 tissue of the wing and is allelic to *blistered*. *Dev. Camb. Engl.* **122**, 2589–2597.
- 471 40. Panfilio KA *et al.* 2019 Molecular evolutionary trends and feeding ecology 472 diversification in the Hemiptera, anchored by the milkweed bug genome. *Genome* 473 *Biol.* **20**, 64. (doi:10.1186/s13059-019-1660-0)
- 41. Emms DM, Kelly S. 2015 OrthoFinder: solving fundamental biases in whole genome comparisons dramatically improves orthogroup inference accuracy. *Genome Biol.* **16**, 157. (doi:10.1186/s13059-015-0721-2)
- 42. Chesebro J, Hrycaj S, Mahfooz N, Popadić A. 2009 Diverging functions of Scr between embryonic and post-embryonic development in a hemimetabolous insect, Oncopeltus fasciatus. Dev. Biol. **329**, 142–151. (doi:10.1016/j.ydbio.2009.01.032)
- 43. Medved V, Marden JH, Fescemyer HW, Der JP, Liu J, Mahfooz N, Popadić A. 2015 Origin and diversification of wings: Insights from a neopteran insect. *Proc. Natl.* 482 *Acad. Sci.* **112**, 15946–15951. (doi:10.1073/pnas.1509517112)
- 44. Tomoyasu Y, Arakane Y, Kramer KJ, Denell RE. 2009 Repeated co-options of exoskeleton formation during wing-to-elytron evolution in beetles. *Curr. Biol.* **19**, 2057–2065. (doi:10.1016/j.cub.2009.11.014)
- 486 45. Morgan TH. 1919 *The Physical Basis of Heredity*. Philadelphia, J. B. Lippincott.
- 46. Williams JA, Bell JB, Carroll SB. 1991 Control of *Drosophila* wing and haltere development by the nuclear *vestigial* gene product. *Genes Dev.* **5**, 2481–2495. (doi:10.1101/gad.5.12b.2481)
- 47. Jockusch EL, Smith FW. 2015 Hexapoda: comparative aspects of later
 embryogenesis and metamorphosis. In *Evolutionary Developmental Biology of Invertebrates 5: Ecdysozoa III: Hexapoda* (ed A Wanninger), pp. 111–208. Vienna:
 Springer. (doi:10.1007/978-3-7091-1868-9 3)

- 48. Kim J, Sebring A, Esch JJ, Kraus ME, Vorwerk K, Magee J, Carroll SB. 1996 Integration of positional signals and regulation of wing formation and identity by *Drosophila vestigial* gene. *Nature* **382**, 133–138. (doi:10.1038/382133a0)
- 49. Halder G, Polaczyk P, Kraus ME, Hudson A, Kim J, Laughon A, Carroll S. 1998 The Vestigial and Scalloped proteins act together to directly regulate wing-specific gene expression in *Drosophila*. *Genes Dev.* **12**, 3900–3909.
- 500 (doi:10.1101/gad.12.24.3900)
- 50. Niwa N, Akimoto-Kato A, Niimi T, Tojo K, Machida R, Hayashi S. 2010 Evolutionary origin of the insect wing via integration of two developmental modules: New hypothesis of insect wing evolution. *Evol. Dev.* **12**, 168–176. (doi:10.1111/j.1525-142X.2010.00402.x)
- 505 51. Edgecombe GD. 2020 Arthropod origins: integrating paleontological and molecular evidence. *Annu. Rev. Ecol. Evol. Syst.* **51**, 1–25. (doi:10.1146/annurev-ecolsys-011720-124437)
- 508 52. O'Donnell BC, Jockusch EL. 2010 The expression of *wingless* and Engrailed in
 509 developing embryos of the mayfly *Ephoron leukon* (Ephemeroptera:
 510 Polymitarcyidae). *Dev. Genes Evol.* 220, 11–24. (doi:10.1007/s00427-010-0324-6)
- 53. Damen WGM, Saridaki T, Averof M. 2002 Diverse adaptations of an ancestral gill: a common evolutionary origin for wings, breathing organs, and spinnerets. *Curr. Biol.* **12**, 1711–1716. (doi:10.1016/s0960-9822(02)01126-0)
- 514 54. Bruce H. 2021 The *Daphnia* carapace and the origin of novel structures. *Prepr.* 515 *Prepr.* (doi:10.20944/preprints202102.0221.v1)
- 55. Cubas P, Celis JF de, Campuzano S, Modolell J. 1991 Proneural clusters of achaete-scute expression and the generation of sensory organs in the *Drosophila* imaginal wing disc. *Genes Dev.* **5**, 996–1008. (doi:10.1101/gad.5.6.996)
- 56. Hu Y, Moczek AP. 2021 Wing serial homologues and the diversification of insect outgrowths: insights from the pupae of scarab beetles. *Proc. R. Soc. B Biol. Sci.* **288**, 20202828. (doi:10.1098/rspb.2020.2828)
- 57. Monteiro A. 2021 Distinguishing serial homologs from novel traits: Experimental limitations and ideas for improvements. *BioEssays* **43**, 2000162. (doi:10.1002/bies.202000162)
- 525 58. Hu Y, Schmitt-Engel C, Schwirz J, Stroehlein N, Richter T, Majumdar U, Bucher G. 2018 A morphological novelty evolved by co-option of a reduced gene regulatory network and gene recruitment in a beetle. *Proc. R. Soc. B Biol. Sci.* **285**, 20181373. (doi:10.1098/rspb.2018.1373)

- 59. Ober KA, Jockusch EL. 2006 The roles of *wingless* and *decapentaplegic* in axis and appendage development in the red flour beetle, *Tribolium castaneum*. *Dev. Biol.* **294**, 391–405. (doi:10.1016/j.ydbio.2006.02.053)
- 60. Ohde T, Mito T, Niimi T. 2021 A wing growth organizer in a hemimetabolous insect suggests wing origin. *bioRxiv* , 2021.03.10.434860.
 (doi:10.1101/2021.03.10.434860)
- 535 61. Clark-Hachtel C. 2021 Pers. comm.

536 Tables

537 Table 1

538

539

540

541

542

543

544

545

546

Sample sizes and frequency of abnormal phenotypes in relevant characters for each RNAi treatment. N is the number of adults scored; only individuals that successfully eclosed to adulthood or could be removed from their final exuvium were scored. Results from different dsRNA fragments targeting the same gene are combined. Negative control specimens were injected alongside each experimental injection batch and have been tabulated together. supr. lobes-supracoxal lobes; pro.-pronotum; f. wings-forewings; h. wings-hind wings; pl. margins-pleural margins.

gene	N	supr. Iobes	collar	pro.	f. wings	h. wings	scutellum	pl. margins	wing hinges
control	319	1%	2%	3%	3%	4%	4%	2%	2%
ар	86	12%	23%	73%	80%	62%	81%	63%	69%
ara/caup	54	24%	11%	31%	6%	0%	31%	4%	0%
hth	76	71%	67%	76%	29%	47%	82%	74%	53%
mirr	37	19%	27%	95%	59%	65%	92%	97%	68%
nub	51	90%	22%	57%	92%	84%	39%	88%	65%
srf	52	88%	88%	94%	92%	73%	94%	92%	83%
tio	50	82%	90%	86%	58%	56%	94%	84%	80%
tup	59	2%	31%	53%	17%	12%	86%	15%	2%
ush	46	0%	17%	59%	22%	15%	48%	46%	20%
vg	48	4%	6%	96%	62%	81%	98%	88%	92%

Figure Legends

547 Figure 1

Cuticularized bilayered epithelia (indicated by dashed lines and blue shading) include multiple thoracic body-wall regions in (a) *Oncopeltus fasciatus*, the large milkweed bug, and fore- and hind wings in *O. fasciatus* and (b) *Drosophila melanogaster*. Credit: Pest and Diseases Images Library, Bugwood.org, used with permission.

Figure 2.

548

549

550

551

552

553

554

555

556

557

558

559

560

561

562

563

564

565

566

567

568

569

570

RNAi effects on wings in *O. fasciatus*; wings are oriented with proximal to the left and the dorsal surface up, unless otherwise specified; the forewing is on top and the hind wing below. (a) Diagram of normal wing morphology. (b) GFP RNAi wings. (c, d) srf RNAi forewing; note three-dimensional 'blistered' phenotype. (d) same forewing rotated to show depth of the blistered wing blade. (e) ap RNAi; pigmentation reduced or lost throughout the forewing, including in the veins (white arrowhead); loss of corium pigmentation (white asterisk) was accompanied by loss of leathery texture. (f) nub RNAi; note smaller wings, with greater reduction proximally in both length and width, resulting in shortened clavus and anal lobe (white asterisks) and indentation anteriorly between corium and membranous forewing (white arrowhead). (g) vg RNAi; note reduced wing size, including clavus and anal lobe, curved (rather than angled) junction of clavus to rest of wing (black arrowhead), pigmentation defects (white asterisks), and distal fusions in forewing venation (white arrowhead). (h) hth RNAi; note altered concave (rather than convex or straight) anterior wing edges proximally (white arrowheads), narrower hind wing blade, and absence of anal lobe (black asterisk). (i) mirr RNAi resulted in a curved junction of clavus and anal lobe (partially torn) to rest of wing (white arrowheads). (j) tup RNAi; forewing narrower with localized reduction in

572

573

574

575

576

577

578

579

580

581

582

583

584

585

586

587

588

589

590

591

592

593

pigment (white asterisk). Scale bar = 5 mm in (b) applies to all panels. Abbreviations: al, anal lobe; cl, clavus; co, corium.

Figure 3.

RNAi effects on dorsal thoracic body-wall in *O. fasciatus*. Dorsal view with right forewing removed; same specimens as in Fig. 2, 4. (a) Diagram of normal dorsal bodywall morphology. (b) GFP RNAi. (c) srf RNAi; all bilayered body-wall evaginations, including the scutellum (white asterisk) and pronotum (black arrowhead), showed a blistered phenotype. (d) ap RNAi; collar reduced, creating gap between collar and eyes (white arrowhead); posterior pronotal margin less defined (white arrow). (e) nub RNAi produced a narrower (black arrowhead) and shorter pronotum, creating gap with eyes (white arrowhead) and exposing normally hidden mesonotal regions (white arrow). (f) vg RNAi; posterior pronotum margin reduced, exposing normally hidden mesonotal regions (white arrow); scutellum broadened posteriorly (white asterisk), with curved lateral edges. (g) ara/caup RNAi; collar reduced (white arrowhead); pronotum shortened; lateral edges of scutellum bent (white asterisk). (h) hth RNAi; collar reduced (white arrowhead); pronotum ventrally curled exposing mesonotal structures (white arrow); scutellum broadened (white asterisk). (i) mirr RNAi; pronotum narrow laterally and curled under posteriorly, exposing wing base (black arrowhead) and mesonotal structures (white arrow); scutellum shorter and narrower (white asterisk). Collar phenotype not present in this specimen. (j) tup RNAi; collar reduced (white arrowhead); lateral pronotal lobes less sculpted (white arrows); scutellum severely reduced (white asterisk) and lacking midline ridge. (k) tio RNAi; widespread body-wall defects, including reduced collar (white arrowhead), reduction in posterior pronotum exposing mesonotal

structures (white arrow); reduced scutellum, with expanded, multilobed posterior edge (white dashed line). (*I*) ush RNAi; reduced collar (white arrowhead); reduced posterior pronotum exposing mesonotal structures (white arrow); scutellum reduced and lacking midline ridge (white asterisk). Scale bar in b = 1 mm (applies to all panels).

Abbreviations: c, collar; fw, forewing; hw, hind wing; sct, scutellum; pn, pronotum; pp, posterior pronotal lobe.

Figure 4.

594

595

596

597

598

599

600

601

602

603

604

605

606

607

608

609

610

611

612

613

614

615

616

RNAi effects on the thoracic pleuron in *O. fasciatus*. Specimens viewed laterally with right forewing removed. (a) Diagram of normal dorsal body-wall morphology. (b) GFP RNAi; note the relatively straight profiles of the pronotum and scutellum (blue dashed lines) and rounded corner at dorsoposterior edge of m3 (white dashed line). (c) srf RNAi; all bilayered body-wall evaginations including the posterior pronotum (white asterisk), pleural lobes (white arrows), and supracoxal lobes (black arrowheads) showed a blistered phenotype. (d) ap RNAi; posterior pleural margins reduced; reduction in m1 reveals underlying mesothoracic wing base (white arrow); reduced melanin near pleural margins (white arrowheads); scutellum up-turned distally (white asterisk). (e) nub RNAi; posterior pleural margins reduced (white arrowheads); reduction in m1 exposes wing base (white arrow); m3 with a more rounded dorsoposterior edge; supracoxal clefts more open (black arrowheads). (f) vg RNAi; reduced junction between the dorsal pronotum and lateral propleuron (white arrow); pronotum appears crumpled in profile (white asterisks); scutellum shortened and with a more rounded posterior tip (black arrowhead). (g) ara/caup RNAi; posterior pleural margins reduced (white arrowheads); m3 with a more rounded dorsoposterior edge;

618

619

620

621

622

623

624

625

626

627

628

629

630

631

632

633

634

635

636

637

638

639

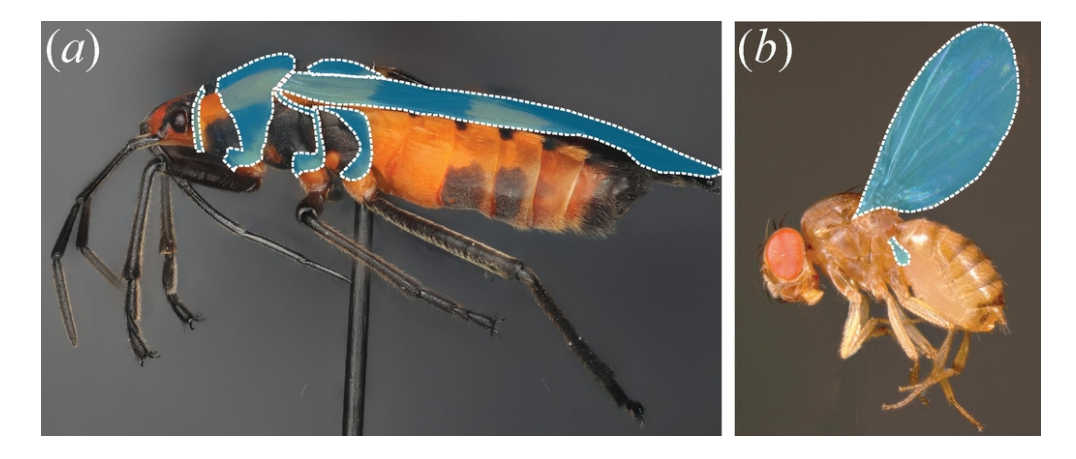
supracoxal clefts more open (black arrowheads); pronotum appears crumpled in profile (white asterisk). (h) hth RNAi; posterior pleural margins reduced (white arrowheads); m3 with a more rounded dorsoposterior edge; pronotum crumpled in profile (white asterisk). (i) *mirr* RNAi, specimen angled slightly, showing more of dorsum than in other specimens; pleural margins reduced (white arrowheads); m3 with a more rounded dorsoposterior edge; pronotum and scutellum appear crumpled in profile (white asterisks). (j) tup RNAi; scutellum reduced and crumpled in profile (white asterisk); loss of pigmentation and sclerotization in pleural margins (white arrowheads). (k) tio RNAi; severe reduction in all thoracic bilayered evaginations; smaller pleural plates (white arrowheads), open supracoxal clefts (black arrowhead); pronotum and scutellum appear crumpled in profile (white asterisks). (I) ush RNAi; posterior pleural margins reduced (white arrowheads); pronotum and scutellum appear crumpled in profile (white asterisks). Scale bar (in b) = 1 mm (applies to all panels). Abbreviations: c, collar; j, junction of pronotum and propleuron; m. margin of posterior pleural lobe, number designates thoracic segment; pn, pronotum; sct, scutellum; sq, scent groove; sl, supracoxal lobe, number designates thoracic segment; wg, wing groove.

Figure 5.

Summary of RNAi effects on thoracic characters. (a) Dorsal and (b) lateral views of normal anatomy with bilayered evaginations shaded; single-layered regions of the body wall are unshaded. (c) Graphical summary of the results of RNAi on the seven main bilayered thoracic characters for the ten genes in this study; shading shows penetrance (proportion of scorable individuals in which the specified character was affected); full opacity represents 100% penetrance. Abbreviations: c, collar; m, pleural

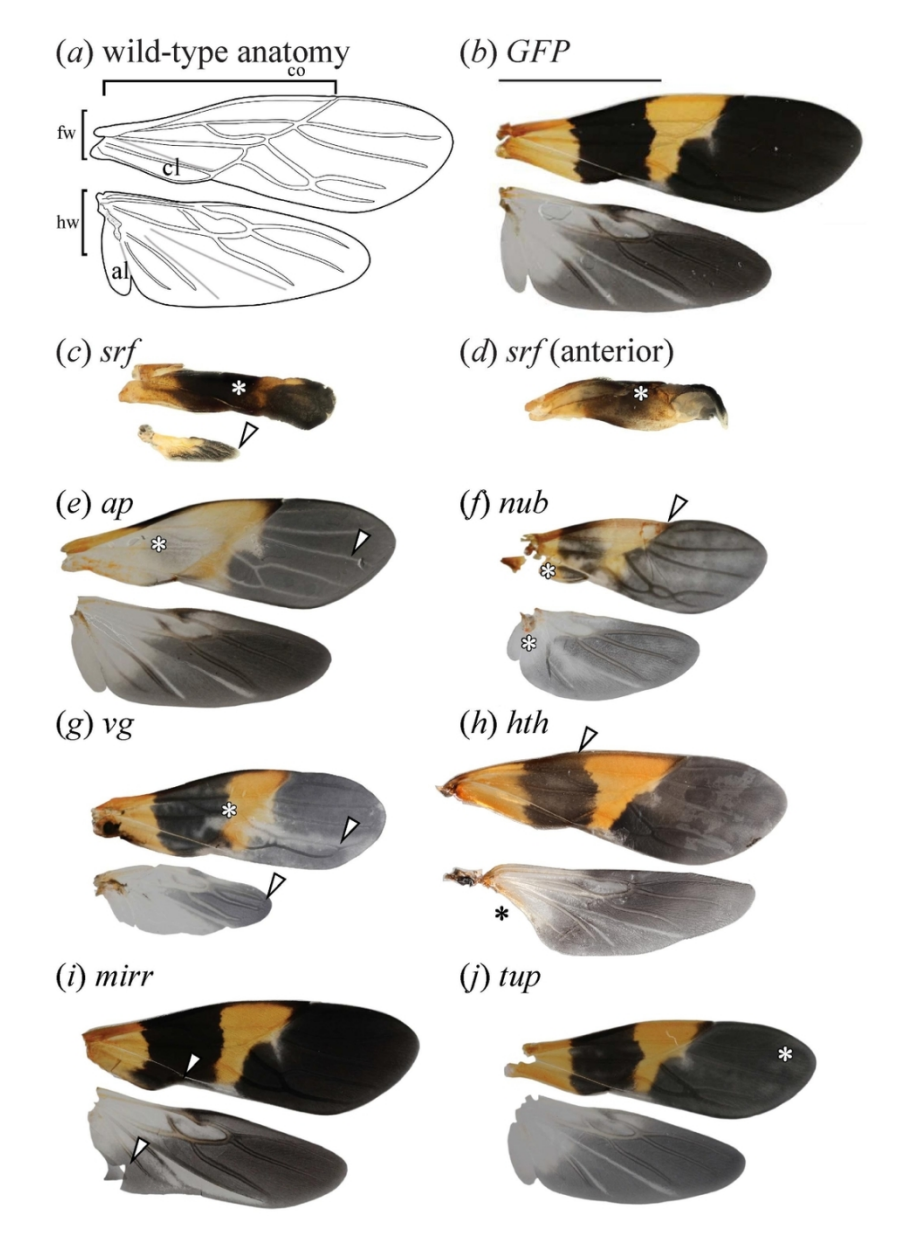
margins, with subscripts denoting thoracic segment; pn, pronotal lobe; j, junction of
pronotum and propleuron; sl, supracoxal lobes, with subscripts denoting thoracic
segment; sct, scutellar lobe; w, wing (including wing hinge).

641



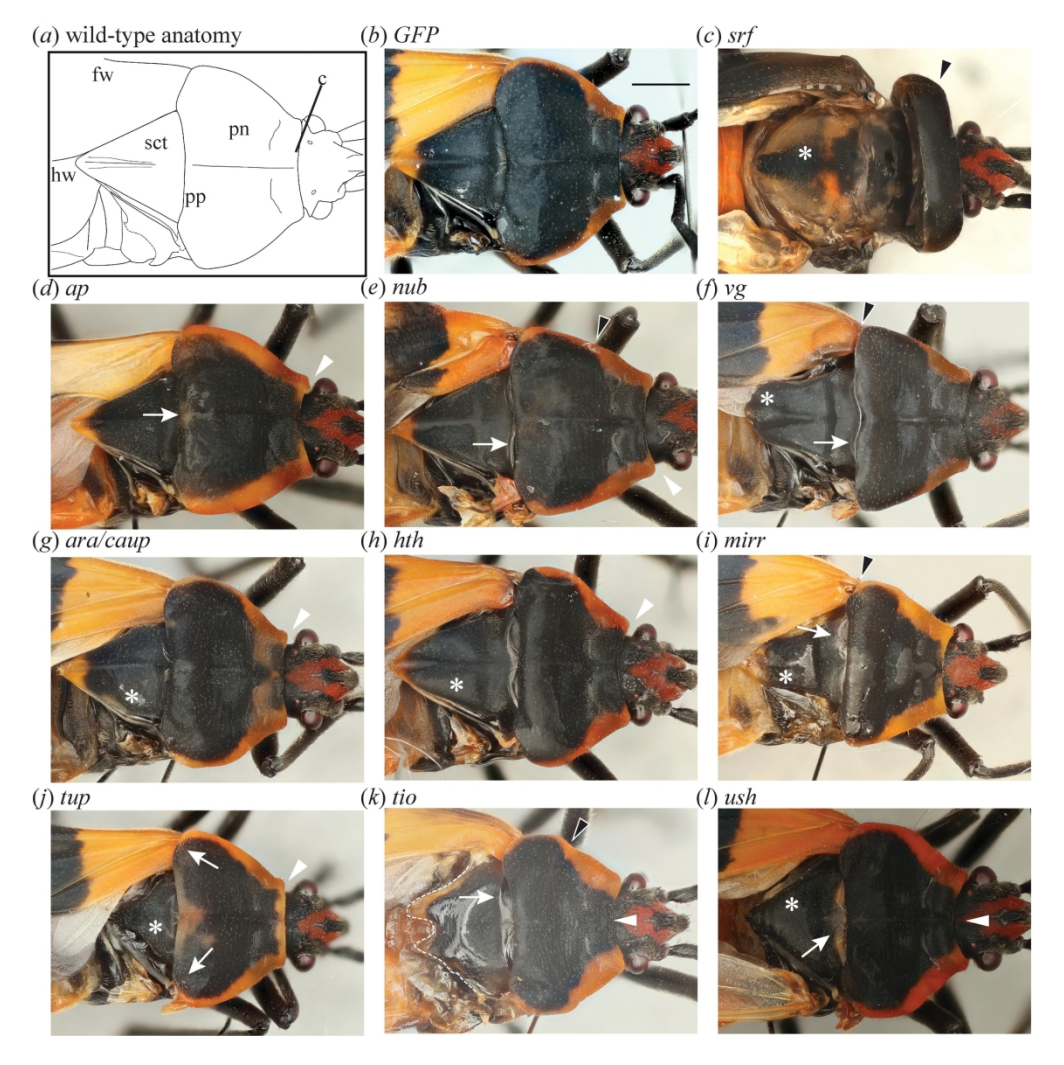
Cuticularized bilayered epithelia (indicated by dashed lines and blue shading) include multiple thoracic bodywall regions in (a) Oncopeltus fasciatus, the large milkweed bug, and fore- and hind wings in O. fasciatus and (b) Drosophila melanogaster. Credit: Pest and Diseases Images Library, Bugwood.org, used with permission.

87x36mm (300 x 300 DPI)



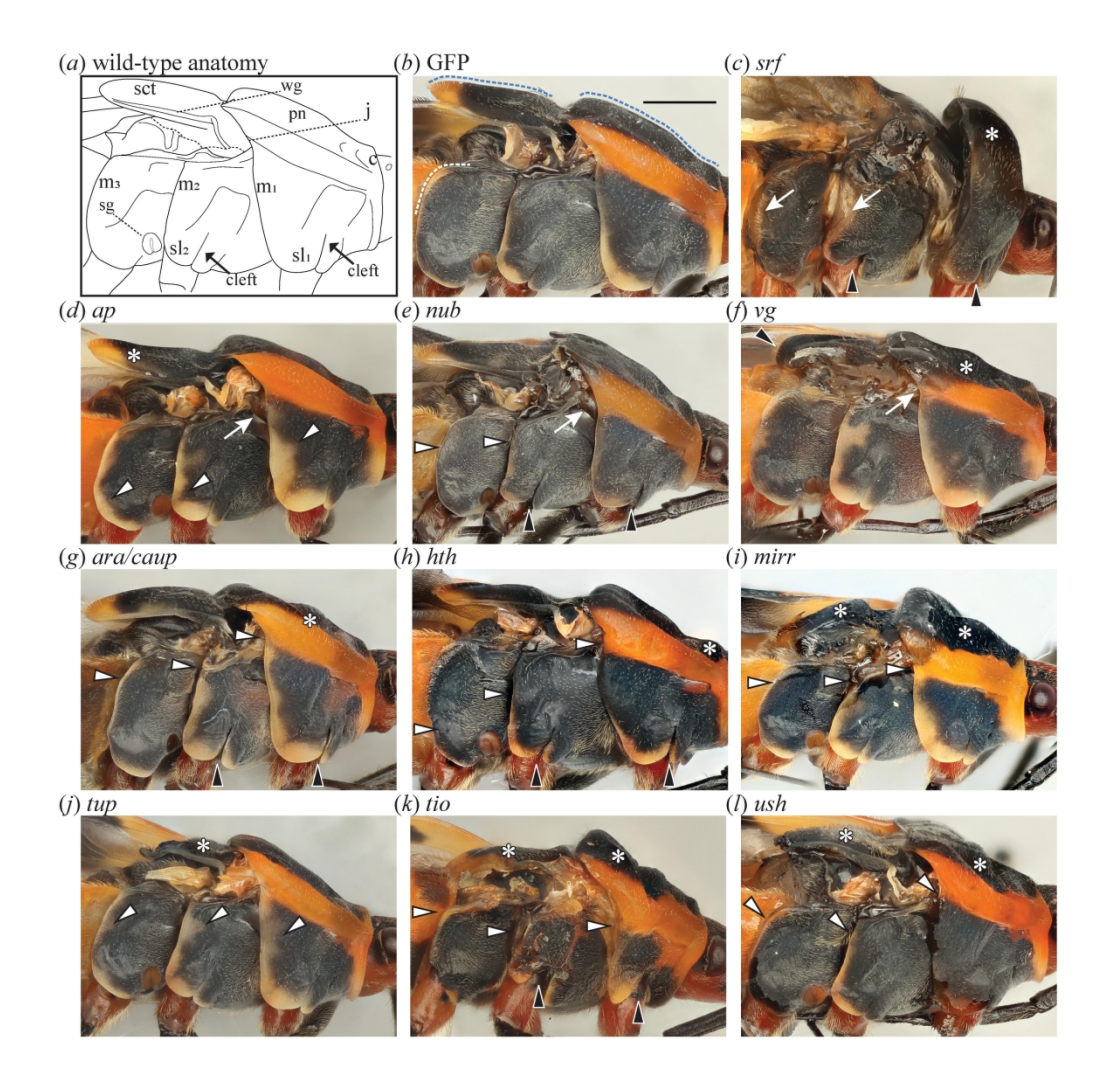
RNAi effects on wings in O. fasciatus; wings are oriented with proximal to the left and the dorsal surface up, unless otherwise specified; the forewing is on top and the hind wing below. (a) Diagram of normal wing morphology. (b) GFP RNAi wings. (c, d) srf RNAi forewing; note three-dimensional 'blistered' phenotype. (d) same forewing rotated to show depth of the blistered wing blade. (e) ap RNAi; pigmentation reduced or lost throughout the forewing, including in the veins (white arrowhead); loss of corium pigmentation (white asterisk) was accompanied by loss of leathery texture. (f) nub RNAi; note smaller wings, with greater reduction proximally in both length and width, resulting in shortened clavus and anal lobe (white asterisks) and indentation anteriorly between corium and membranous forewing (white arrowhead). (g) vg RNAi; note reduced wing size, including clavus and anal lobe, curved (rather than angled) junction of clavus to rest of wing (black arrowhead), pigmentation defects (white asterisks), and distal fusions in forewing venation (white arrowhead). (h) hth RNAi; note altered concave (rather than convex or straight) anterior wing edges proximally (white arrowheads), narrower hind wing blade, and absence of anal lobe (black asterisk). (i) mirr RNAi resulted in a curved junction of clavus and anal lobe (partially torn) to rest of wing (white arrowheads). (j) tup RNAi; forewing narrower with localized reduction in pigment (white asterisk). Scale bar = 5 mm in

(b) applies to all panels. Abbreviations: al, anal lobe; cl, clavus; co, corium. 87x127mm~(300~x~300~DPI)



RNAi effects on dorsal thoracic body-wall in O. fasciatus. Dorsal view with right forewing removed; same specimens as in Fig. 2, 4. (a) Diagram of normal dorsal body-wall morphology. (b) GFP RNAi. (c) srf RNAi; all bilayered body-wall evaginations, including the scutellum (white asterisk) and pronotum (black arrowhead), showed a blistered phenotype. (d) ap RNAi; collar reduced, creating gap between collar and eyes (white arrowhead); posterior pronotal margin less defined (white arrow). (e) nub RNAi produced a narrower (black arrowhead) and shorter pronotum, creating gap with eyes (white arrowhead) and exposing normally hidden mesonotal regions (white arrow). (f) vg RNAi; posterior pronotum margin reduced, exposing normally hidden mesonotal regions (white arrow); scutellum broadened posteriorly (white asterisk), with curved lateral edges. (g) ara/caup RNAi; collar reduced (white arrowhead); pronotum shortened; lateral edges of scutellum bent (white asterisk). (h) hth RNAi; collar reduced (white arrowhead); pronotum ventrally curled exposing mesonotal structures (white arrow); scutellum broadened (white asterisk). (i) mirr RNAi; pronotum narrow laterally and curled under posteriorly, exposing wing base (black arrowhead) and mesonotal structures (white arrow); scutellum shorter and narrower (white asterisk). Collar phenotype not present in this specimen. (j) tup RNAi; collar reduced (white arrowhead); lateral pronotal lobes less sculpted (white arrows); scutellum severely reduced (white asterisk) and lacking midline ridge. (k) tio RNAi; widespread body-wall defects, including reduced collar (white arrowhead), reduction in posterior pronotum exposing mesonotal structures (white arrow); reduced scutellum, with expanded, multilobed posterior edge (white dashed line). (I) ush RNAi; reduced collar (white arrowhead); reduced posterior pronotum exposing mesonotal structures (white arrow); scutellum reduced and lacking midline ridge (white asterisk). Scale bar in b = 1 mm (applies to all panels). Abbreviations: c, collar; fw, forewing;

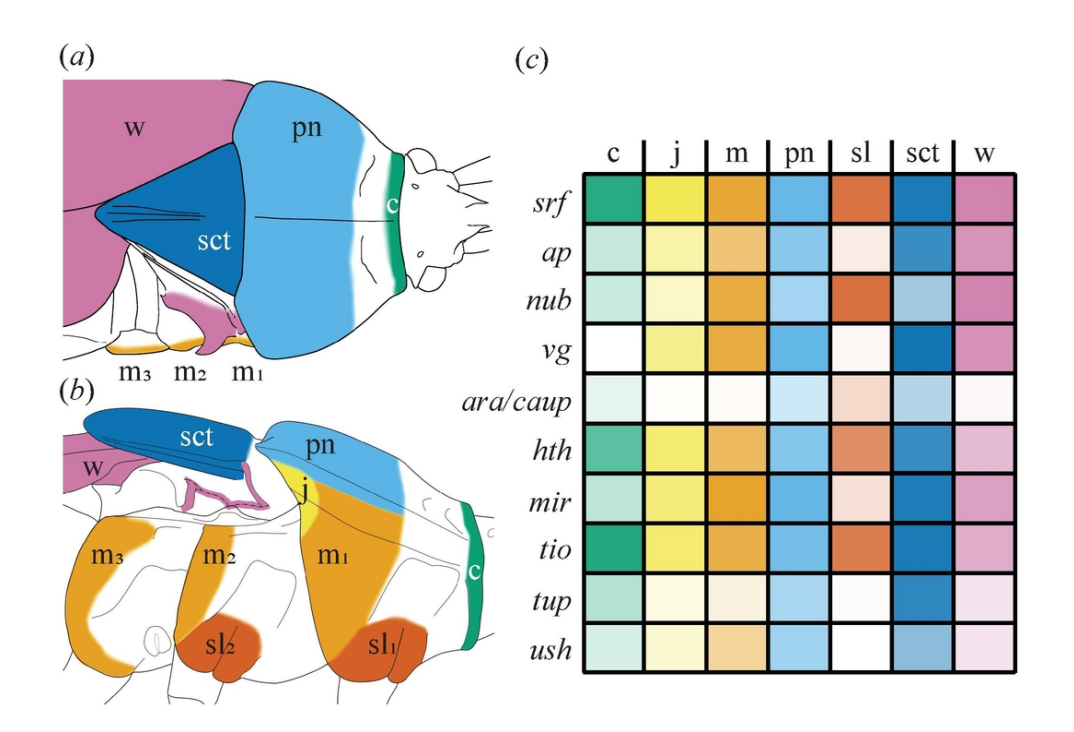
hw, hind wing; sct, scutellum; pn, pronotum; pp, posterior pronotal lobe. $180 x 182 mm \; (300 \; x \; 300 \; DPI)$



RNAi effects on the thoracic pleuron in O. fasciatus. Specimens viewed laterally with right forewing removed. (a) Diagram of normal dorsal body-wall morphology. (b) GFP RNAi; note the relatively straight profiles of the pronotum and scutellum (blue dashed lines) and rounded corner at dorsoposterior edge of m3 (white dashed line). (c) srf RNAi; all bilayered body-wall evaginations including the posterior pronotum (white asterisk), pleural lobes (white arrows), and supracoxal lobes (black arrowheads) showed a blistered phenotype. (d) ap RNAi; posterior pleural margins reduced; reduction in m1 reveals underlying mesothoracic wing base (white arrow); reduced melanin near pleural margins (white arrowheads); scutellum up-turned distally (white asterisk). (e) nub RNAi; posterior pleural margins reduced (white arrowheads); reduction in m1 exposes wing base (white arrow); m3 with a more rounded dorsoposterior edge; supracoxal clefts more open (black arrowheads). (f) vg RNAi; reduced junction between the dorsal pronotum and lateral propleuron (white arrow); pronotum appears crumpled in profile (white asterisks); scutellum shortened and with a more rounded posterior tip (black arrowhead). (g) ara/caup RNAi; posterior pleural margins reduced (white arrowheads); m3 with a more rounded dorsoposterior edge; supracoxal clefts more open (black arrowheads); pronotum appears crumpled in profile (white asterisk). (h) hth RNAi; posterior pleural margins reduced (white arrowheads); m3 with a more rounded dorsoposterior edge; pronotum crumpled in profile (white asterisk). (i) mirr RNAi, specimen angled slightly, showing more of dorsum than in other specimens; pleural margins reduced (white arrowheads); m3 with a more rounded dorsoposterior edge; pronotum and scutellum appear crumpled in profile (white asterisks). (j) tup RNAi; scutellum reduced and crumpled in profile (white asterisk); loss of pigmentation and sclerotization in pleural margins (white arrowheads). (k) tio RNAi; severe reduction in all thoracic bilayered evaginations; smaller pleural plates (white arrowheads),

open supracoxal clefts (black arrowhead); pronotum and scutellum appear crumpled in profile (white asterisks). (I) ush RNAi; posterior pleural margins reduced (white arrowheads); pronotum and scutellum appear crumpled in profile (white asterisks). Scale bar (in b) = 1 mm (applies to all panels). Abbreviations: c, collar; j, junction of pronotum and propleuron; m, margin of posterior pleural lobe, number designates thoracic segment; pn, pronotum; sct, scutellum; sg, scent groove; sl, supracoxal lobe, number designates thoracic segment; wg, wing groove.

180x184mm (300 x 300 DPI)



Summary of RNAi effects on thoracic characters. (a) Dorsal and (b) lateral views of normal anatomy with bilayered evaginations shaded; single-layered regions of the body wall are unshaded. (c) Graphical summary of the results of RNAi on the seven main bilayered thoracic characters for the ten genes in this study; shading shows penetrance (proportion of scorable individuals in which the specified character was affected); full opacity represents 100% penetrance. Abbreviations: c, collar; m, pleural margins, with subscripts denoting thoracic segment; pn, pronotal lobe; j, junction of pronotum and propleuron; sl, supracoxal lobes, with subscripts denoting thoracic segment; sct, scutellar lobe; w, wing (including wing hinge).

91x63mm (300 x 300 DPI)